Frustration and Self-Ordering of Topological Defects in Ferroelectrics

Y. Nahas,* S. Prokhorenko, and L. Bellaiche
Physics Department and Institute for Nanoscience and Engineering, University of Arkansas, Fayetteville, Arkansas 72701, USA
(Received 28 July 2015; published 18 March 2016)

A first-principles-based effective Hamiltonian technique is used to investigate the interplay between geometrical frustration and the ordering of topological defects in a ferroelectric nanocomposite consisting of a square array of $BaTiO_3$ nanowires embedded in a $Ba_{0.15}Sr_{0.85}TiO_3$ matrix. Different arrangements of the wires' chiralities geometrically frustrate the matrix, which in response exhibits point topological defects featuring self-assembled ordered structures spatially fluctuating down to the lowest temperatures. These fluctuations thereby endow the system with residual configurational entropy from which many properties characteristic of geometric frustration, such as the ground state degeneracy and the broadness of the dielectric response, are further found to originate.

DOI: 10.1103/PhysRevLett.116.117603

Frustration generally arises whenever a given physical system is subjected to incompatible requirements which inhibit the formation of a uniquely defined and homogeneously ordered ground state configuration [1–3]. Under competing influences, the full development of correlation is hindered, and rather than a long-range order, a pronounced tendency for complex spatial organization consisting of the juxtaposition of short-range correlated regions and defective regions occurs. Geometrical frustration is an inevitable feature of a wide variety of systems [4–10] and has focused considerable interest on the unusual phenomena it prompts, among which are spin ice and spin liquid phases [11–13]. Unlike the frustration inherent to disordered systems such as spin glasses wherein competing interactions fail to be simultaneously satisfied [14–16], geometrical frustration can manifest in well-defined structures as a result of the incompatibility between the geometry of the latter and the interactions governing the collective behavior of a set of degrees of freedom. Only recently geometrical frustration has been suggested to occur in ferroelectrics [17,18] and many of its important aspects (discovered in other types of materials) remain to be investigated. These include, for instance, the examination of chirality as a frustration inducing mechanism, and the emergence of self-assembled ordered patterns of topological defects as a frustration accommodating response [8,10,19].

In this Letter, we inquire how chirality competes with geometrical constraints within a ferroelectric nanocomposite system consisting of a square array of $BaTiO_3$ (BTO) nanowires embedded in a $Ba_{0.15}Sr_{0.85}TiO_3$ matrix. Note that these two materials are ferroelectric in their bulk form. We find that, as a result of the weak coupling between the chiralities of the wires, independent choices of chiral symmetry breaking in each of the wires geometrically constrains the matrix to incompatible orientational boundary conditions. The evaluation of the frustration index from the dielectric susceptibility substantiates the geometrical frustration the system is subjected to. We further topologically characterize the local accommodation of the resulting geometrical frustration, and find that the matrix features a self-assembled ordered structure of vortices and antivortices. Such structures spatially fluctuate down to the lowest temperatures, thereby indicating the existence of a residual entropy at the origin of the ground state degeneracy and other features of geometrical frustration.

The considered nanocomposite structure is depicted in Fig. 1. This nanocomposite is mimicked by a $32 \times 32 \times 6$ supercell that is periodic along the x, y, and z axis (which lie along the pseudocubic [100], [010], [001] directions, respectively). Its properties are predicted by performing Monte Carlo simulations (using at least 100000 sweeps) of the first-principles-based effective Hamiltonian scheme of Ref. [20], which has been shown to accurately reproduce various (static and dynamical) properties of different disordered or chemically-ordered $(Ba, Sr)TiO_3$ systems [17,20–24]. Methodological details are provided in the

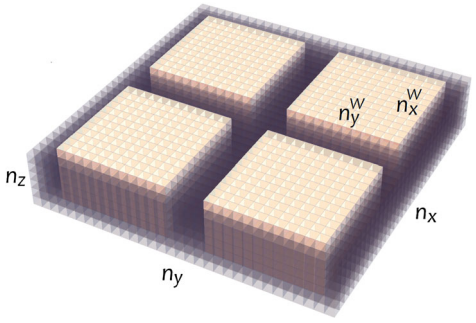

FIG. 1. Schematic representation of the periodic supercell under study. The structure consists of four BTO nanowires of cross-sectional dimension $n_x^W = n_y^W = 12$ lattice constant units ($\sim$21.4 nm^2) separated by 4 lattice constant units and embedded in a $Ba_{0.15}Sr_{0.85}TiO_3$ matrix with lateral sides along the [100] and [010] directions of $n_x = n_y = 32$ lattice constant units, and a length $n_z = 6$ along the [001] pseudocubic direction.

Supplemental Material [25]. A primary feature of this type of nanocomposite is the occurrence within each of the wires of a chiral symmetry breaking which stabilizes a flux-closure domain structure enclosing a vortex at its core and coexisting with a spontaneous polarization along the axial direction of the nanowires [24]. Such chiral occurrence was further predicted to spontaneously exhibit natural optical activity [30], unusual electronic properties, and peculiar collective atomic vibrations associated with THz dynamics of electrical vortices [31,32]. Moreover, the growth of such nanocomposite structures constitutes an active experimental area. Nanocomposites that are very similar to the ones investigated here, namely, nanowires embedded in a matrix or diphasic composites with (1-3) connectivity pattern, were successfully formed [33]. Also, synthesis of single crystalline ferroelectric nanowires composed of ternary perovskite oxides ($BaTiO_3$ and $SrTiO_3$) [34,35], as well as fabrication of nanoarrays of dielectric wires and nanopillars embedded in a $BaTiO_3$ matrix [36,37], have already been described. The choice of such a nanostructure is thus motivated by the advancement in the controlled growth of composites with tailored functionalities [38], and the wide variety of novel behaviors they feature (note, however, that the growth of low-dimensional perovskites within a perovskite matrix remains a difficult task to experimentally achieve).

In our search for the ground state configuration(s) of the considered nanocomposite, we have examined the four possible relative arrangements of the wires' chiralities. The manually initiated configurations $C1$, $C2$, $C3$, and $C4$ combined clockwise (+) and anticlockwise (−) circulation direction of the cross-sectional polarization around the vortex core enclosed in each of the wires, with $C1$: $[++++]$, $C2$: $[--+-]$, $C3$: $[--++]$, and $C4$: $[-+-+]$, where the sequence of circulations refers to the top-left, top-right, bottom-left, and bottom-right wires, respectively. These configurations were subsequently relaxed at 5 K. The resulting relaxed configurations feature a spontaneous polarization along the axial direction of the nanowire, co-occurring with flux-closure four-domain vortex structures of the cross-sectional polarization field in each of the wires with the assigned circulation. The latter in-plane vortex pattern within the wires corresponds to a tangential ordering against the interfaces whereby the depolarizing field experienced by the in-plane components is reduced [39]. We find that the (1-3) connectivity [33] of the considered nanocomposite structure hosts a polarization state possessing *translational invariance* along the axial direction of the wire. The polarization field thus depends only on x and y spatial coordinates, enabling a visualization of the system as consisting of two-dimensional layers (z planes). The corresponding cross-sectional polarization fields are shown in Fig. 2 which displays the x and y components of the electric dipoles in an arbitrary (001) plane of the periodic supercell for each of the four configurations $C1$, $C2$, $C3$, and $C4$. It is

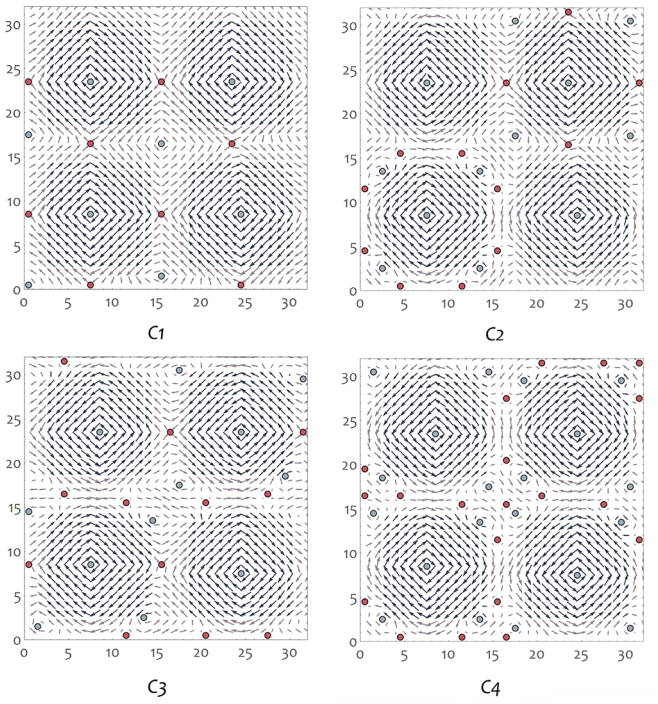

FIG. 2. Microstructure (in-plane component of local modes and defects distribution) for the configurations $C1$: $[++++]$, $C2$: $[--+-]$, $C3$: $[--++]$, and $C4$: $[-+-+]$ at 5 K. Blue (red) circles denote vortices (antivortices). Dark (light) arrows indicate the dipoles lying in the wires (matrices).

therein seen that the different patterns of the wires' chiralities endow the matrix with complex microstructures, which is a characteristic feature exhibited by systems affected by geometrical frustration [1–3].

Also shown in Fig. 2 are the location of point topological defects. The lattice form of the O(2) winding number [40] characterizing the topological defects associated with the two-dimensional cross-sectional polarization field is constructed as follows. Each xy plane of the supercell is a square lattice composed of elementary plaquettes. In order to assign a topological charge to each of the plaquettes, a counterclockwise orientation is first chosen. Each set of four normalized projections of local dipoles is then mapped onto the unit circle. We identify the shortest arc between the neighboring dipoles and depending on whether the circle is covered counterclockwise or clockwise, the enclosed defect is a vortex (of charge +1) or an antivortex (charge −1). If the circle is not covered, the plaquette is defect-free.

These four relaxed configurations appear to be stable with nearly identical low-lying energies, as a result of the weak interaction between the chirality of different wires [41]. Taking $C1$ as the reference energy, the simulations yielded energy differences of 0.76 meV, 0.86 meV, and 1.55 meV per unit cell for $C2$, $C3$, and $C4$, respectively. We moreover found that annealing the system from a cold start yielded one or the other of these configurations as a ground state. Remarkably, this result stands as further indication of a

chirality-induced frustration since it points to a quasifourfold ground state degeneracy and the suppression of a conventional long range order within the cross-sectional polarization fields [1,2]. Given the discrepancy between the wires and matrix polarizabilities, independent choices of chiral symmetry breaking first occur in each of the wires, geometrically constraining the matrix to incompatible orientational boundary conditions. As a result, the matrix fails to analytically interpolate between the wires and features instead strong fluctuations in its cross-sectional dipolar field. These strong fluctuations concentrate distortions and are found to encompass singularities or topological defects, enabling the surrounding medium to be locally ordered, i.e., allowing the utmost extent of the orientational correlations dictated by the wires beyond their strict periphery. These topological defects are necessary components of ground states. Strikingly, they emerge in a self-assembled ordered array as it is best seen in configuration $C4$ in Fig. 2, where vortices and antivortices adopt a staggered ordering. Interestingly, such ordered structures with periodic arrays of defects have already been characterized as an expression of geometric frustration in various systems such as chiral liquid crystals [10,42], the antiferromagnetic rotator model [43], and the spin nematic model on a triangular lattice [44], but never in ferroelectrics, to the best of our knowledge. Let us note that self-assembling structures on length scales that are difficult to obtain by standard techniques spur interest in the conception of new materials with advanced functionalities [45,46]. Moreover, it is worth noticing that configuration $C1$ with its pattern of vortices and antivortices has been experimentally observed in magnetic systems [47], which implies that our subsequent discussion could lead to the further investigation of geometrical frustration in the phase-locked magnetic state [47].

One of the most revealing properties of a geometrically frustrated system lies in the dependence on temperature, T, of its susceptibility [1–3]. Specifically, a frustration index f can be defined as the ratio of θ_{CW}, the Curie-Weiss temperature, to the transition temperature. At high temperatures, the susceptibility follows the Curie-Weiss law and its inverse is a straight line, $\chi^{-1} \propto T - \theta_{\mathrm{CW}}$. In conventional systems devoid of frustration, a single anomaly in χ occurs at a temperature $T \sim \theta_{\mathrm{CW}}$, accordingly to mean-field expectations. In contrast, within geometrically frustrated systems, a departure from this expectation occurs, and f is found to deviate from unity. This deviation is imputed to the prolongation of the paraphase to temperatures lower than θ_{CW} whereby fluctuations are only very weakly correlated and the behavior of susceptibility is close to the Curie-Weiss law [1]. In order to evaluate the frustration index f of the presently considered case of a ferroelectric nanocomposite, it is first worth noting that we are in the presence of at least two phase transitions that can be put in direct correspondence with topological defects of the cross-sectional polarization field. Upon cooling from high temperatures, the wires acquire a nonzero value of the z component of their toroidal moment around 330 K (not shown), thereby signaling the appearance of a circulating pattern of the cross-sectional polarization field and the condensation of vortices at their core. This first transition is accompanied by a very small cusp in the in-plane susceptibility [24]. On further decreasing temperature, a second cusp, much more pronounced, is featured by the in-plane susceptibility at $T_{\mathrm{ord}} \sim 75$ K. This second transition is ascribable to the matrix as it signals the temperature below which its number of vortices and antivortices is conserved, and their positions relatively defined.

The evolution with temperature of the inverse in-plane susceptibility $\chi_\perp = (\chi_{11} + \chi_{22})/2$ is obtained upon heating configurations $C1$, $C2$, $C3$, and $C4$. In order to probe the effect of the spacing between wires on the frustration, we further inquire into the temperature dependence of $\chi_\perp$ for a configuration that we denote by $C1'$, solely differing from $C1$ in the spacing between its nanowires, 6 instead of 4 lattice constant units. Configuration $C1'$ is thus obtained within a $36 \times 36 \times 6$ supercell where the cross-sectional dimension of the wires is kept unchanged ($n_x^W = n_y^W = 12$ lattice constant units). The dielectric susceptibility tensor is practically calculated as in Refs. [48,49]. In Fig. 3(a) we

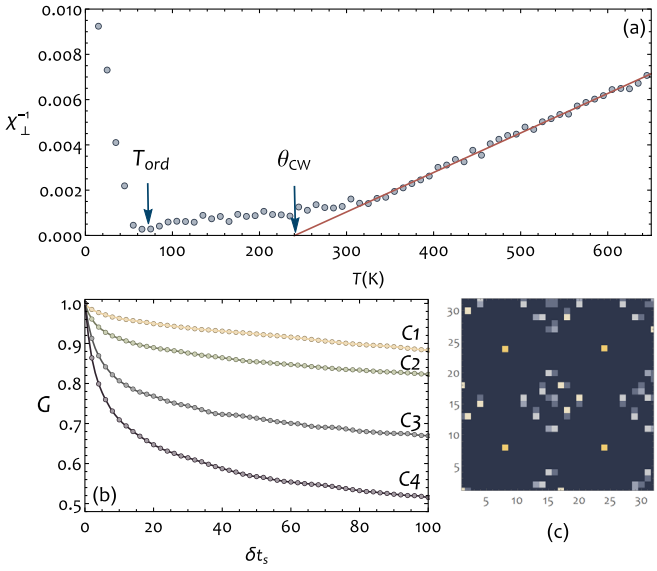

FIG. 3. (a) Temperature dependence of the inverse in-plane susceptibility $\chi_\perp^{-1}$ corresponding to configuration $C1'$. Vertical arrows indicate the transition temperature at which vortices and antivortices order in the matrix (T_{ord}), and the Curie-Weiss temperature (θ_{CW}). Red line is a linear fit of the high temperature values of $\chi_\perp^{-1}$. (b) Monte Carlo time autocorrelation function $G(\delta t_s)$ of the spatial distribution of topological defects (vortices and antivortices) for configurations $C1$, $C2$, $C3$, and $C4$ at 5 K. (c) Spatial probability distribution of defects at 5 K for configuration $C4$. Yellow to dark blue gradient color indicates high to low probability of occurrence. The data is statistically gathered from 5000 sweeps, after the initial constructed structure has been allowed to relax by performing 100000 MC sweeps.

show as an example $\chi_\perp^{-1}$ for configuration $C1'$. Linearly fitting the high temperature values of $\chi_\perp^{-1}$ yields a fitting parameter θ_{CW} of 240 K, thus allowing an estimate of the frustration index, $f = \theta_{CW}/T_{ord}$. We find $f = 3.2$ which attests of the system being geometrically frustrated. In particular, the quasilinear regime featured by $\chi_\perp^{-1}$ starting from θ_{CW} and down to T_{ord} unequivocally indicates that it is the matrix that primarily experiences the frustration, as its dipoles retain the ability to almost freely fluctuate below θ_{CW}. This latter observation is in line with the prolongation of a paraphase down to temperatures well below θ_{CW} [1,2]. In the same manner, we estimate the frustration index from $\chi_\perp^{-1}$ for each of $C1$, $C2$, $C3$, $C4$, and find $f = 3.09$, $f = 3.13$, $f = 3.68$, and $f = 4.03$, respectively, thus indicating that the antiferrotoroidic arrangement of chiralities is the most frustrated one ($C4$) and that widening the matrix results in an increase of frustration ($C1'$ versus $C1$).

Among the most striking features of a geometrically frustrated system is the residual entropy at the origin of its ground state degeneracy [1–3]. We address this question by resorting to a Monte Carlo time autocorrelation function of the spatial distribution of topological defects in the matrix over sweeps. The adopted formula of the normalized Monte Carlo time autocorrelation function is such that $G(\delta t_s)$ is equal to

$$\frac{1}{\rho_T N(s-\delta t_s)} \sum_{t_s,i} \delta[W(t_s,i), W(t_s+\delta t_s,i)] \qquad (1)$$

where t_s is the Monte Carlo sweep, $\rho_T N$ is the average number of defects at temperature T, s is the number of sweeps, and where the delta symbol $\delta[W(t_s,i), W(t_s+\delta t_s,i)]$ assigns 0 or 1 according to whether or not the spatial distribution W of topological defects over the sites i at times t_s and $t_s+\delta t_s$ differ. G provides a measure for the extent throughout which similarity persists between two spatial configurations, and thus allows us to quantitatively estimate the free volume accessible to the defects in the matrix. It is computed for the well-thermalized configurations $C1$, $C2$, $C3$, and $C4$ at 5 K [Fig. 3(b)]. Whereas we find that the vortices enclosed in the wires remain pinned at definite positions ($G = 1$ for the vortices of the wires, not shown), defects in the matrix spatially fluctuate, as indicated by the drop of G. These results demonstrate that many configurations with quasi-identical energies (the standard deviation of the energies per unit cell is of the order of 10^{-5} eV) are reachable for each of the $C1$, $C2$, $C3$, and $C4$ chirality arrangements, thereby pointing to a nonvanishing entropy for $T \to 0$, i.e., to the existence of a residual entropy. We note that the drop of $G(\delta t_s)$ is not identical among the four configurations, and that it is maximal for configuration $C4$ enabling the identification of this configuration as the most frustrated of the four, consistently with the frustration index f whose value is maximal for configuration $C4$. Moreover, from the above we can infer that the dependence of the degree of frustration on the ground state degeneracy scales with the free volume accessible to the defects of the matrix, and thus attribute f's increase of $C1'$ with respect to $C1$ to the loosening of the confinement of the matrix defects as a result of the enlargement of the spacing between the wires. We show in Fig. 3(c) the spatial probability distribution of defects for $C4$ at 5 K, gathered from statistics on 5000 sweeps. While it is seen that the vortices enclosed by the wires are pinned at their center, the ordered array of vortices and antivortices in the matrix exhibits a floating character [50], at the origin of the drop of G.

In the event of the occurrence of defects such as dislocations, point defects, space charges, etc., some of the discussed features of geometrical frustration may be affected. As a result of inhomogeneous mechanical and electrical fields arising from these defects, some chiral configurations may be precluded, thereby possibly, partially lifting the quasi-fourfold ground state degeneracy ($C1$, $C2$, $C3$, $C4$), and modifying the matrix dipolar microstructures. Dislocations, for instance, are known to induce pinning effects on vortices' cores in ferroelectrics [51], which can facilitate their nucleation while possibly altering the orderly and floating characters of vortice and antivortice self-assembly. Nonetheless, in magnetic systems where the involved energies are likewise small, the $C1$ configuration has been experimentally observed [47].

On another note, ferroelectric films perforated by a two-dimensional lattice of cylindrical holes [52] bear a similarity to the nanocomposite structure explored here while likely being easier to fabricate. Such film topology can give rise to vortices and complex dipolar microstructures, thereby constituting a possible alternative route to investigating the effect of a depolarizing field in entailing geometric frustration.

In summary, investigating a chiral ferroelectric nanocomposite consisting of a square array of BTO nanowires embedded in a less polarizable matrix, we have found that independent choices of chiral symmetry breaking in each of the wires geometrically constrain the matrix to incompatible orientational boundary conditions. Assessment of the frustration index based on the dielectric susceptibility attests of the geometrical frustration the system is subjected to. In response to the frustration, the matrix locally accommodates such orientational incompatibilities by featuring a self-assembled ordered structure of vortices and antivortices. Such structures are found to fluctuate while preserving the energy, thereby pointing to a residual entropy at the origin of the ground state degeneracy.

We thank L. Louis for providing initial data on different arrangements of the wires' chiralities. This work is supported by the ARO Grant No. W911NF-12-1–0085. S. P. and L. B. are also thankful for the financial support of DARPA Grant No. HR0011-15-2-0038 (MATRIX program).

*yousra.nahas@gmail.com

[1] R. Moessner and A. P. Ramirez, Phys. Today **59**, 24 (2006).
[2] J. T. Chalker, in *Introduction to Frustrated Magnetism*, Springer Series in Solid-State Sciences Vol. 164 (Springer, Berlin/Heidelberg, 2011), pp 3–22.
[3] A. P. Ramirez, Annu. Rev. Mater. Sci. **24**, 453 (1994).
[4] L. Pauling, J. Am. Chem. Soc. **57**, 2680 (1935).
[5] M. J. Harris, S. T. Bramwell, D. F. McMorrow, T. Zeiske, and K. W. Godfrey, Phys. Rev. Lett. **79**, 2554 (1997).
[6] S. T. Bramwell and M. J. P. Gingras, Science **294**, 1495 (2001).
[7] R. Moessner, Can. J. Phys. **79**, 1283 (2001).
[8] A. P. Ramirez, Nature (London) **421**, 483 (2003).
[9] P. W. Anderson, Science **235**, 1196 (1987).
[10] R. D. Kamien and J. V. Selinger, J. Phys. Condens. Matter **13**, R1 (2001).
[11] A. P. Ramirez, A. Hayashi, R. J. Cava, R. Siddharthan, and B. S. Shastry, Nature (London) **399**, 333 (1999).
[12] P. Chandra and B. Doucot, Phys. Rev. B **38**, 9335(R) (1988).
[13] L. Balents, Nature (London) **464**, 199 (2010).
[14] G. Toulouse, Commun. Phys. **2**, 115 (1997).
[15] D. Chowdhury, in *Spin Glasses and Other Frustrated Systems* (World Scientific, Singapore, 1986), p. 231.
[16] K. Binder and A. P. Young, Rev. Mod. Phys. **58**, 801 (1986).
[17] N. Choudhury, L. Walizer, S. Lisenkov, and L. Bellaiche, Nature (London) **470**, 513 (2011).
[18] R. Xu, S. Liu, I. Grinberg, J. Karthik, A. R. Damodaran, A. M. Rappe, and L. W. Martin, Nat. Mater. **14**, 79 (2015).
[19] M. Udagawa and Y. Motome, J. Phys. Conf. Ser. **200**, 012214 (2010).
[20] L. Walizer, S. Lisenkov, and L. Bellaiche, Phys. Rev. B **73**, 144105 (2006).
[21] S. Lisenkov and L. Bellaiche, Phys. Rev. B **76**, 020102(R) (2007).
[22] J. Hlinka, T. Ostapchuk, D. Nuzhnyy, J. Petzelt, P. Kuzel, C. Kadlec, P. Vanek, I. Ponomareva, and L. Bellaiche, Phys. Rev. Lett. **101**, 167402 (2008).
[23] Q. Zhang and I. Ponomareva, Phys. Rev. Lett. **105**, 147602 (2010).
[24] L. Louis, I. A. Kornev, G. Geneste, B. Dkhil, and L. Bellaiche, J. Phys. Condens. Matter **24**, 402201 (2012).
[25] See Supplemental Material at http://link.aps.org/supplemental/10.1103/PhysRevLett.116.117603 for methodological details, which includes Refs. [26–29]
[26] W. Zhong, D. Vanderbilt, and K. M. Rabe, Phys. Rev. B **52**, 6301 (1995).
[27] L. Bellaiche and D. Vanderbilt, Phys. Rev. B **61**, 7877 (2000).
[28] N. J. Ramer and A. M. Rappe, J. Phys. Chem. Solids **61**, 315 (2000).
[29] L. Bellaiche, A. Garcia, and D. Vanderbilt, Phys. Rev. Lett. **84**, 5427 (2000).
[30] S. Prosandeev, A. Malashevich, Z. Gui, L. Louis, R. Walter, I. Souza, and L. Bellaiche, Phys. Rev. B **87**, 195111 (2013).
[31] Z. Gui, L.-W. Wang, L. Bellaiche, and Bellaiche, Nano Lett. **15**, 3224 (2015).
[32] Z. Gui and L. Bellaiche, Phys. Rev. B **89**, 064303 (2014).
[33] R. E. Newnham, D. P. Skinner, and L. E. Cross, Mater. Res. Bull. **13**, 525 (1978).
[34] J. J. Urban, W. S. Yun, Q. Gu, and H. Park, J. Am. Chem. Soc. **124**, 1186 (2002).
[35] W. S. Yun, J. J. Urban, Q. Gu, and H. Park, Nano Lett. **2**, 447 (2002).
[36] S. Karthauser, E. Vasco, R. Dittmann, and R. Waser, Nanotechnology **15**, S122 (2004).
[37] H. Zheng, J. Wang, S. E. Lofland, Z. Ma, L. Mohaddes-Ardabili, T. Zhao, L. Salamanca-Riba, S. R. Shinde, S. B. Ogale, F. Bai, D. Viehland, Y. Jia, D. G. Schlom, M. Wuttig, A. Roytburd, and R. Ramesh, Science **303**, 661 (2004).
[38] C. A. F. Vaz, J. Hoffman, C. H. Ahn, and R. Ramesh, Adv. Mater. **22**, 2900 (2010).
[39] S. Prosandeev and L. Bellaiche, Phys. Rev. Lett. **97**, 167601 (2006).
[40] N. D. Mermin, Rev. Mod. Phys. **51**, 591 (1979).
[41] S. Prosandeev and L. Bellaiche, Phys. Rev. B **75**, 094102 (2007).
[42] M. B. Pandey, P. J. Ackerman, A. Burkart, T. Porenta, S. Zumer, and Ivan I. Smalyukh, Phys. Rev. E **91**, 012501 (2015).
[43] S. Miyashita and H. Shiba, J. Phys. Soc. Jpn. **53**, 1145 (1984).
[44] H. Tsunetsugu and M. Arikawa, J. Phys. Soc. Jpn. **75**, 083701 (2006).
[45] A. Imhof and D. J. Pine, Nature (London) **389**, 948 (1997).
[46] M. Park, C. Harrison, P. M. Chaikin, R. A. Register, and D. H. Adamson, Science **276**, 1401 (1997).
[47] A. Ruotolo, V. Cros, B. Georges, A. Dussaux, J. Grollier, C. Deranlot, R. Guillemet, K. Bouzehouane, S. Fusil, and A. Fert, Nat. Nanotechnol. **4**, 528 (2009).
[48] A. Garcia and D. Vanderbilt, in *First-Principles Calculations For Ferroelectrics: Fifth Williamsburg Workshop*, edited by R. E. Cohen (AIP, Woodbury, New York, 1998), p. 53.
[49] K. Rabe and E. Cokayne, in *First-Principles Calculations for Ferroelectrics: Fifth Williamsburg Workshop*, edited by R. E. Cohen (AIP, Woodbury, New York, 1998), p. 61.
[50] M. Franz and S. Teitel, Phys. Rev. B **51**, 6551 (1995).
[51] W. J. Chen, Y. Zheng, and B. Wang, Appl. Phys. Lett. **104**, 222912 (2014).
[52] A. P. Levanyuk, I. B. Misirlioglu, E. D. Mishina, and A. S. Sigov, Phys. Solid State **54**, 2243 (2012).